



Biocomposites from porcine plasma protein and urban parks and gardens green waste

Carlos Bengoechea^{a,*}, Ana Paula Batista^b, Estefanía Álvarez-Castillo^a, Antonio Guerrero^a, Nathalie Gontard^b, Helene Angellier-Coussy^b

^a Departamento de Ingeniería Química, Universidad de Sevilla, Escuela Politécnica Superior, Calle Virgen de África, 7, 41011 Sevilla, Spain

^b Joint Research Unit IATE Agropolymers Engineering & Emerging Technology, INRAE, University Montpellier, Institut Agro, CIRAD, 2, Place Pierre Viala, 34060 Montpellier, France

ARTICLE INFO

Keywords:

Plasma protein
Urban green waste
Biocomposite
Dry fractionation
Lignocellulosic filler

ABSTRACT

Biorefinery was used to transform two organic wastes, i.e. urban park & garden green waste and porcine plasma (PPP), into raw materials for biocomposite production. The effect of the nature, size and content of the filler on the final performance of biocomposites was assessed. Two fractions stemming from an urban park and garden green waste, i.e. a representative fraction of the total waste (RF) and a branches-rich fraction (B), were considered as fillers of a PPP bioplastic. PPP-RF/B biocomposites were obtained by compression-moulding and then characterised by tensile tests, dynamic mechanical analysis, water uptake, and water vapour permeability. Using a filler size around 28 μm at 30 wt%, the Young's Modulus of samples including B fraction was double the value of that including RF, due to the presence of grass in the overall urban waste. Moreover, a greater strengthening was perceived when using larger particle sizes (around 140 μm) of the B fraction, highlighting the importance of the grinding stage. The loss tangent evolution with temperature from dynamic mechanical tests denoted an antiplasticizing effect of the urban biowastes, which should be considered in future applications as a certain exudation degree would be expected. Regarding barrier properties, water permeability increased at higher filler contents (i.e., 30 wt%), while oxygen permeability decreased.

Generally, composites from plasma and urban biowaste could be considered in future applications (e.g., packaging), as they showed great reinforcement and stability during water immersion, apart from a darker tonality and decreased oxygen permeability.

1. Introduction

Despite the global rise in environmental awareness, there is still no completely satisfactory ecological alternative to conventional non-biodegradable plastics, mostly used in single-use applications (e.g., food packaging). During the last decades, many authors have focused on the manufacture of biodegradable and/or biobased plastics from different types of biomass looking for adequate properties to compete with conventional petrochemical plastics (Mohanty et al., 2005; Rhim et al., 2013; Verbeek and van den Berg, 2010). The spread of these green plastic materials in the market would help mitigate the negative environmental impact of the polymer industry, mainly associated with their accumulation in landfills and their dependence on non-renewable fossil resources. In a circular economy framework, organic waste from

different industrial activities has been tested as raw material for the development of greener plastics (Abascal and Regan, 2018) in different sectors, such as packaging (Kriegel et al., 2008; Razzaq et al., 2016), superabsorbent pads (Álvarez-Castillo et al., 2020a; Cuadri et al., 2017), horticulture (Jiménez-Rosado et al., 2018), drug release (Elzoghby et al., 2012) or biomedicine (Jiménez and González-Muñiz, 2019).

An important volume of blood resulting from animal slaughterhouses is discharged directly into the environment annually, which is problematic due to its high pollutant load (Álvarez et al., 2012; Bah et al., 2013; Lynch et al., 2017). However, its high protein content (~ 90%) promotes recovery and reuse, as suggested by the European Union's fundamental waste management principles (The European Parliament and the Council of the European Union, 2008), that would valorise this by-product of the meat industry (Peters, 1975; Piot et al., 1986). Blood is

* Corresponding author.

E-mail address: cbengoechea@us.es (C. Bengoechea).

¹ Departamento de Ingeniería Química, Universidad de Sevilla, Escuela Politécnica Superior, 41012 Sevilla (Spain), Fax: +34 954557179

commonly separated by centrifugation into different fractions: red cells, platelets and plasma. Plasma is a mixture of water and proteins (50–60% of serum albumin, 40–50% of α , β , γ globulins and 1–3% of fibrinogen) (Dávila et al., 2007). It is currently used as a water-holding agent in some food products, an emulsifier or even as a replacer of other food ingredients, such as egg albumen, in certain formulations (Hurtado et al., 2012, 2011; Raeker and Johnson, 1995). The overproduction of blood, which results in the discarding of the majority (~ 70%), has promoted the study of the feasibility of producing bioplastic materials from plasma protein through conventional plastic processing techniques. Thus, biopolymers from biowaste (e.g. from the meat industry) have been successfully processed by different manufacturing techniques, such as casting (Ashter, 2016; Nuthong et al., 2009a), extrusion (Uitto et al., 2020), injection moulding (Álvarez-Castillo et al., 2019), thermopressing (Viretto et al., 2021) or 3D printing (Álvarez-Castillo et al., 2020c). As glycerol has been extensively reported to have good compatibility with different protein-based sources (Álvarez-Castillo et al., 2021a; Delgado et al., 2018; Fernández-Espada et al., 2016; Perez-Puyana et al., 2016), it has been mostly employed as a plasticizer to facilitate the mobility of polymeric chains, easing their processing.

A huge volume of biodegradable green waste (~150 kg per person in Europe) (Som et al., 2009) is picked up every year from gardens and parks in urban areas, having been identified in the European Waste Catalogue (EWC) by the six-digit code 20 02 01 (Eades et al., 2020). Together with food waste, green waste constitutes the largest fraction of municipal solid waste (Kumar et al., 2010; Wei et al., 2017). It is mainly composed of green and dead leaves, tree bark and wood, branches, grass and soil, among others (Bustamante et al., 2016; Haynes et al., 2015). This residue is mostly underused (MacFarlane, 2009; Reyes-Torres et al., 2018; Vandecasteele et al., 2016) due to its low bulk density, which makes its transfer and transport more expensive. Gardens and parks waste is composed of two main different fractions: a) a coarse fraction, rich in lignocellulosic compounds hardly manageable and with a slow biodegradation (Reyes-Torres et al., 2018); and b) fine fractions, mainly consisting of green leaves and stems which are more easily decomposable (Belyaeva and Haynes, 2009; Haynes et al., 2015). Urban green waste has been mainly reused for composting or co-composting (Francou et al., 2008) and energy production (Kranert et al., 2010; Shi et al., 2013). Viretto et al. (2021) first explored their use as lignocellulosic fillers after dry fractionation, obtaining five different fractions with a particle size of around 100 μm . It was shown that the branches-rich fraction displayed the best reinforcing effect in a polyhydroxybutyrate-co-valerate (PHBV) plastic material, whereas the grasses-rich fraction slightly degraded the overall mechanical performance (Viretto et al., 2021).

Previous works have used lignocellulosic fillers obtained from different low-value sources, such as parks and garden wastes, winery wastes, almond shells, rice husks, or seagrass (David et al., 2020; Sánchez-Safont et al., 2018; Viretto et al., 2021). All those studied were focused on the effect of those fillers on plastics based on a microbial polymer (i.e., PHBV). In this context, the present study focuses on developing and characterizing biodegradable materials based on a widely available organic waste obtained from slaughterhouses (i.e., porcine blood plasma protein), using lignocellulosic fillers derived from urban gardens and parks green waste. To our knowledge, there is no other paper dealing with the analysis of the effect of lignocellulosic fillers in protein-based bioplastics. Composite materials were produced by thermopressing, which consisted in confining in a mould a homogeneous waste-plasticizer blend, and then submitting it to high pressure and temperature, finally giving rise to composites specimens with the desired shape (López-Castejón et al., 2016). Two different lignocellulosic fractions, produced by dry fractionation of urban parks and gardens green waste according to the protocol described by Viretto et al. (Viretto et al., 2021), were used as fillers, i.e. a branches-rich fraction and a representative mixture of the whole residue. Fine particles of these fillers were obtained when ground by an impact mill, which could be

followed by an additional grinding stage in a ball mill, obtaining ultrafine particles of the fillers.

The biocomposites obtained may be used in the packaging or horticultural fields, where biodegradability would be enhanced compared to commonly used materials. Tensile and rheological properties, as well as colour and barrier properties, should be tested regarding their use in those fields. The applicability of plastic materials containing lignocellulosic wastes in the production of packaging (Sánchez-Safont et al., 2018) or horticultural pots (Nechita et al., 2010; Pratibha, Hariprasad, P, 2022) has already been tested. The main goal of the present manuscript was to evaluate the impact of filler composition, particle size and content (up to 30 wt%) on the performance of composite materials based on a protein system (porcine plasma) reinforced with lignocellulosic fillers from urban parks and gardens green waste. In this sense, this manuscript intends to elucidate the properties-structure relation of the materials studied.

2. Materials and methods

2.1. Raw materials

In this study, AproPork porcine plasma protein (PPP) was generously supplied by a local retailer Proanda (Spain). PPP possessed a protein content of around 74%, as determined using a Kjeldhal factor of 6.25 through a LECO CHNS-932 Nitrogen analyser (Leco Corporation, St. Joseph, MI, USA). Furthermore, moisture and ashes content in PPP were respectively around 9% and 17%. Glycerol (99.5%, Pure Chem, USA) was used as plasticizer in every sample. A fully representative sample batch of urban parks and gardens' green waste were collected in July 2017 and provided by the RGS NORDIC composting facility (Copenhagen – Selinevej) in the frame of the H2020 Resurbis project.

2.2. Preparation of lignocellulosic fillers and composites

Lignocellulosic fillers were obtained according to a procedure described previously by Viretto et al. (Viretto et al., 2021). Briefly, the raw biomass was sorted by hand to isolate different valuable fractions: branches, leaves, grasses and small lignocellulosic pieces. After drying at 60 °C overnight, the size of the different sorted fractions was initially reduced by employing a cutting mill type SM100 (Retsch, Germany), passing first on a 4.0 mm sieve and consecutively on a 1.0 mm sieve. Subsequently, those fractions were dried again at 60 °C and then ground at 18,000 rpm on an impact mill type 100UPZ (Hosokawa Alpine, Germany) with a 0.3 mm sieve (trapezoid holes), an 8-teeth rotor and an output recovery cyclone. Fine samples with an apparent median diameter in volume (d_{50}) of around 120–140 μm were targeted at this stage (Viretto et al., 2021). A Representative Fraction (RF) was reconstituted from the different valuable ground fractions to represent the overall sample batch. Thus, the composition of this reconstituted RF sample was: 26 wt% of branches; 6 wt% of leaves; 4 wt% of grasses; 64 wt% of the mixture with soil. Aliquots of the fine branches-rich fraction (B_{fine}) and the fine representative fraction (RF_{fine}) were dried again at 60 °C overnight before being ground to obtain ultra-fine powders (B_{ultra fine} and RF_{ultra fine}) with a targeted value of d_{50} around 20–30 μm . For that purpose, grinding was done using a ball milling type DM1 (Sweco, United States): a 34 L polyurethane abrasion-resistant elastomer lining jar filled with porcelain media. The porcelain media were cylinders (13 mm in diameter and length) and balls (15 mm in diameter) in a 50/50 blend. The internal volume of the jar was occupied as follows: 1/3 for porcelain media (48 kg) and 1/3 for fillers (1 kg).

Composite films were prepared through a three-stage process: a) Blending: initially, the required amounts of the solid ingredients (PPP, filler) were mixed thoroughly by hand using a porcelain mortar and pestle. Once a homogeneous mixture was achieved, the plasticizer (glycerol) was added keeping always the PPP/glycerol ratio at 1/1 and mixed likewise. As the lignocellulosic filler content increased from 0 to

30 wt%, the protein and glycerol content varied at every filler level. Therefore, PPP contents of 50, 47.5, 42.5 and 35 wt% were set for 0, 5, 15 and 30 wt% filler content, respectively; b) Compression moulding: blends were placed on a 10x10x 0.03 cm³ square cavity between two Teflon-coated plates, and then pressed using a hydraulic press (Pinette Emidecau Industries, France) at 150 °C. The pressure was increased gradually up to 150 bar for 3 min and then held constant for 1 min. During the compression of PPP, temperature/pressure promotes protein coagulation and the formation of covalent bonds between protein chains (Álvarez-Castillo et al., 2019). It should be noticed that thermal degradation of lignocellulosic urban fillers or porcine plasma takes place at higher temperatures than the processing temperature of the compressed films (Nuthong et al., 2009b; Viretto et al., 2021); and c) Cutting: films obtained were finally cut onto properly shaped probes (dumbbell, square or circular) using a cutting press (model S1, Wallace Instruments, United Kingdom).

2.3. Methods

2.3.1. Lignocellulosic fillers

2.3.1.1. Particle size. A Mastersizer 2000 (Malvern Instruments Ltd., United Kingdom) determined the particle size distributions of all fillers employed. The particles were dispersed in an ethanol solution (95% (v/v)) and analyzed for obscuration values from 3% to 10%. Refractive indices of 1.47 for lignocellulosic fillers and 1.36 for ethanol were used. For all specimens, three cycles of measurements were performed at ambient temperature and measurements were done in triplicate for each filler fraction. The apparent median diameter d_{50} , as well as the span value ($(d_{10}-d_{90})/d_{50}$), were calculated from distributions in volume.

2.3.1.2. Morphology. The morphology of lignocellulosic particles was examined by scanning electron microscopy (Desktop SEM Phenom ProX (ThermoFisher Scientific, USA)).

2.3.1.3. Calorimetry. An 822 calorimeter (Mettler Toledo, USA) was used to perform Differential Scanning Calorimetry (DSC) tests, using Star System software. Thus, lignocellulosic biowaste was placed in hermetically sealed aluminium pans, and tests were run at a rate of 10 °C/min from -20–300 °C, using an empty pan as a reference.

2.3.2. Biocomposites

2.3.2.1. Morphology. Biocomposite samples were gold coated and observed by Scanning Electron Microscopy (SEM) using a ZEISS EVO (USA) microscope. Micrographs were acquired using a beam current of 11–12 pA at a working distance of 7 mm and with an acceleration voltage of 10 kV. Analyses were carried out with ca. 100x and 1000x magnification.

2.3.2.2. Colour. The colour of compression moulded circular probes of the composites studied was measured using a chroma metre (CR-410, Konica Minolta, Japan), with an 8 mm aperture. The following parameters were assessed: L*(luminosity), a*(red intensity), and b*(yellow intensity), and total colour difference (ΔE^*) was calculated according to Eq. 1.

$$\Delta E = \sqrt{(\Delta L^*)^2 + (\Delta a^*)^2 + (\Delta b^*)^2} \quad (1)$$

Where: ΔE^* is the difference between the Colour parameters of the bioplastic sample and the blank standard (L*: 95.59; a*: -5.56; b*: 8.16).

2.3.2.3. Tensile properties. Mechanical properties of the bioplastics, such as Young's modulus (E), tensile strength (σ_{max}) and deformation at

break (ϵ_{max}), were estimated by performing uniaxial tensile tests until rupture. These tests were carried out at room temperature at a strain rate of 50 mm·min⁻¹ using a texture analyzer (Zwick, Zwick Roell Group, Ulm, Germany). Before their mechanical characterization, dumbbell probes (D-638-03 Type IV) were stored at 0% RH over anhydrous silica gel at room temperature for two days.

2.3.2.4. Dynamic mechanical analysis. Linear viscoelastic properties of the composites were determined through small amplitude oscillatory measurements using rectangular probes (width 10 mm, ISO 178). In a DMTA rheometer (DMA1 STAR System, Mettler Toledo, Switzerland), temperature ramp tests were performed with a 3-point bending geometry from -80 °C to 120 °C at constant frequency (1 Hz) and heating rate (5 °C/min).

2.3.2.5. Water uptake capacity. Composite samples (circular probes with a diameter of 25 mm) were dried at 50 °C for 24 h (w_1), and later immersed in deionised water (w_2) for 24 h; finally, wet samples were dehydrated at 50 °C for 24 h (w_3). Water uptake capacity (WUC) and Soluble Matter Loss (SML) were determined using Eqs. 2 and 3:

$$WUC(\%) = \frac{w_2 - w_3}{w_3} \cdot 100 \quad (2)$$

$$SML(\%) = \frac{w_1 - w_3}{w_1} \cdot 100 \quad (3)$$

2.3.2.6. Water vapour and oxygen permeability. A modified ASTM E96 procedure (ASTM-E96/E96M, 2016) was followed to measure gravimetrically the water vapour permeability (WVP) at 23 °C. Film samples (five replicates) were sealed in permeation chambers where a relative humidity (RH) gradient from 0 (silica gel) to 100% (water) was established, which promotes the permeation of water molecules through the composites. The rate of water vapour movement through the films was calculated by periodic weightings of the permeation cells. WVP (mol·s⁻¹·Pa⁻¹·m⁻¹) was estimated using Eq. 4.

$$WVP = \frac{S \times l}{3600 \times A \times \Delta P \times M_{H_2O}} \quad (4)$$

where S was the slope of the weight change in the linear region (g·h⁻¹), A the film permeation surface area (0.000908 m²), l the average film thickness (m), ΔP the saturation vapour pressure at 23 °C, and M_{H_2O} the molar mass of water (g·mol⁻¹).

The Oxygen Permeability (O₂P) was estimated by an oxygen permeability tester (PreSens, Fibox 4, Germany) at 100% RH and 23 °C. In short, this device placed the composite film between two chambers (three replicates). All the surrounding O₂ was removed using a nitrogen flush on both sides of the films, and then a constant oxygen flow (50 mL/min) was applied to the lower chamber. On the other hand, the upper chamber was hermetically closed. Thus, O₂ molecules could pass by permeation across the sample where the sensor was placed; the device determined the oxygen entrance in % for 4 days. O₂P (mol·s⁻¹·Pa⁻¹·m⁻¹) was determined using Eq. 4:

$$O_2P = \frac{J \times l}{A \times \Delta P} \quad (5)$$

where J is the transmission rate of O₂ (mol·s⁻¹), l is the film thickness (m), A is the film permeation surface area (0.00126 m²), and ΔP is the differential partial pressure of the permeant gas across the film (Pa).

2.4. Statistical analysis

All measurements were carried out at least in triplicate, using Statgraphics software (Statgraphics Technologies, Inc., The Plains, VA, USA) for the statistical analysis. Standard deviations are included for all the parameters determined.

3. Results and discussion

3.1. Description of the fillers

The lignocellulosic fillers employed were branches (B) and a representative fraction (RF) of the whole urban waste considered. The biochemical composition d.b. of those fillers is cellulose (30% (B); 25% (RF)); hemicellulose (30% (B); 16% (RF)); lignin (23% (B); 27% (RF)); extractives (10% (B); 11% (RF)); and ashes (7% (B); 21% (RF)) (Viretto et al., 2021).

Thermograms of both fillers employed in the present study, B and RF, show similar thermal transitions (Fig. 1). Thus, they both show a second-order transition around 127 °C, which can be related to a glass transition, and distinct endothermic peaks around 157, 165, and 195 °C. The presence of different peaks may be related to the heterogeneous composition of the fillers and the slight differences in their location should be caused by differences in their composition. Those endothermic peaks are followed by an exothermic region that has been previously related to lignin (Ufodike et al., 2020). Another peak is observed at around 234 °C for both samples in the exothermic region, which has been also associated with the presence of lignin, cellulose and hemicellulose (Ibbett et al., 2019).

After the corresponding milling stage, the particle size distribution of fine (B_{fine} and RF_{fine}) and ultra-fine powders (B_{ultra fine} and RF_{ultra fine}) used as fillers in the biocomposites was determined by laser light scattering diffraction. The ball milling step allowed a significant reduction of the size of fillers. Thus, apparent diameter d_{50} diminished from $138 \pm 3 \mu\text{m}$ to $23.3 \pm 0.2 \mu\text{m}$ for the branches-rich fraction, and from $117.3 \pm 0.9 \mu\text{m}$ to $33 \pm 3 \mu\text{m}$ for the RF fraction.

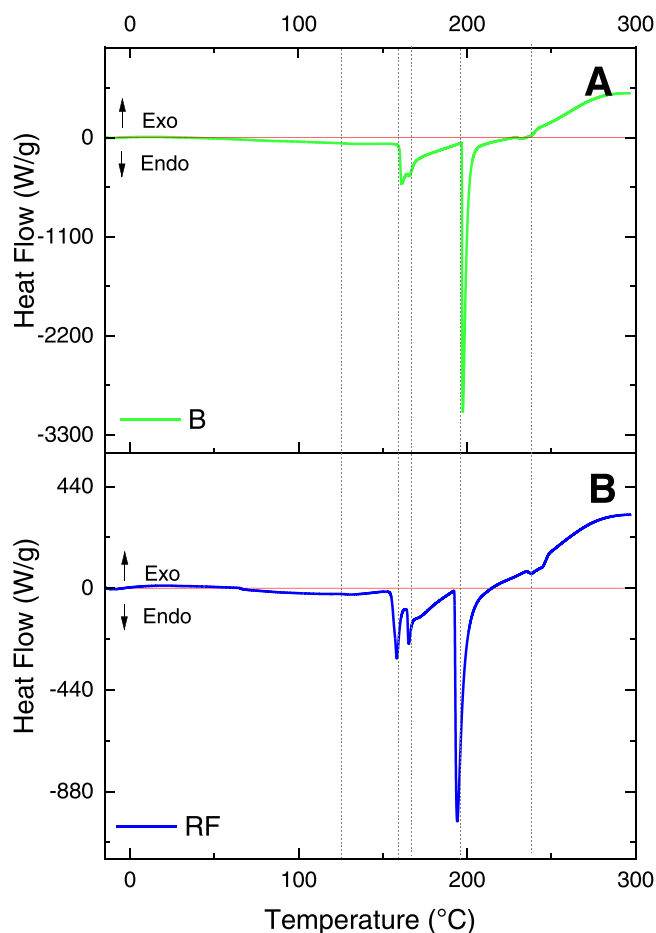


Fig. 1. DSC thermograms for the lignocellulosic fillers: branches (B) and a representative fraction (RF).

The RF fillers issued from ball milling presented a wider volume-based size distribution than the branch fillers, due to the recalcitrance of mineral particles to grinding.

The morphology of lignocellulosic particles was also qualitatively observed by scanning electron microscopy, SEM (Fig. 2). The two branches-rich fractions, B_{fine} and B_{ultra fine}, were characterized by more elongated particles, that seem to be more recalcitrant to grinding. On the other hand, RF_{ultra fine} fillers were more homogeneous in terms of size and shape than B_{ultra fine} fillers.

3.2. Morphology and colour

SEM images (Fig. 3) show the microstructure observed at the surface of bioplastics without any filler (neat PPP) and with 30% of each of the lignocellulosic fillers considered (B_{fine}, B_{ultra fine}, RF_{ultra fine}). In any case, the roughness of the surface is increased when fillers are included. A slight difference is observed between different fillers with similar diameters as B_{ultra fine} shows a surface slightly rougher than RF_{ultra fine}. However, the biocomposite including B_{fine}, which possesses a larger particle size, is the one that shows a more remarkable heterogeneous morphology and with a worse filler dispersion, displaying fibrillar microstructures along the whole surface. This should be related to less effective interaction between components (Berthet et al., 2015). In general, the morphology of the surface of the composite might be determined to be more dependent on the particle size than on the fraction of filler used by those studied.

The predominant colour of the composites was brown and its intensity depended noteworthy on the content of the lignocellulosic bio-waste used as filler. Films became darker as the filler content increased from 0 to 30 wt%. Moreover, composites including the fraction with the largest size (B_{fine}) were visibly more heterogeneous and presented a rougher surface than those including ultra-fine fractions with smaller sizes. Colour differences were supported by the ΔE^* values and changes in colour parameter values (L, a^* , b^*) (Table 1). When differences are perceivable at a glance, they are reported to display ΔE^* values equal to 5 or higher when compared with the control system (0 wt% filler).

Both b^* and a^* parameters decreased as the filler content increased. While b^* indicates chromatic differences from yellowness (positive values) to blueness (negative values), a^* indicates chromatic differences from redness (positive values) to greenness (negative values) (Technical Committee 1, 48, 2004). The red (a^*) dominance in the control sample should be attributed to blood plasma (i.e., haemoglobin), which was masked by the inclusion of the lignocellulosic fillers in the biocomposites. Slighter differences could be observed in the lightness (L parameter) of the samples, displaying only noteworthy differences when solely branches were used as fillers at the greatest level contents.

Other works have reported differences in the colour of plasma protein films when using different plasticizers and processed at different temperatures (Nuthong et al., 2009c) or when phenolic compounds were added (Nuthong et al., 2009b), proving that composition is an essential parameter determining the colour of plastic materials. There are packaging or horticultural applications where transparency or light-coloured materials are not mandatory, such as food trays or pots.

3.3. Mechanical properties

Fig. 4 shows the stress-deformation curves obtained through uniaxial tests until the break of the samples. All the samples displayed the typical tensile behaviour of thermoplastic polymers. The Young's modulus (E) was calculated from the initial slope, while the tensile strength (σ_{max}) and the strain at break were recorded at the fracture of the material (Fig. 5).

Globally, introducing lignocellulosic fillers in PPP resulted in brittle and rigid materials, as highlighted respectively by the strong decrease of the strain at break (from 82.4% for the neat matrix down to 5.3% for PPP filled with 30 wt% of B_{fine}) and the increase of Young's modulus from

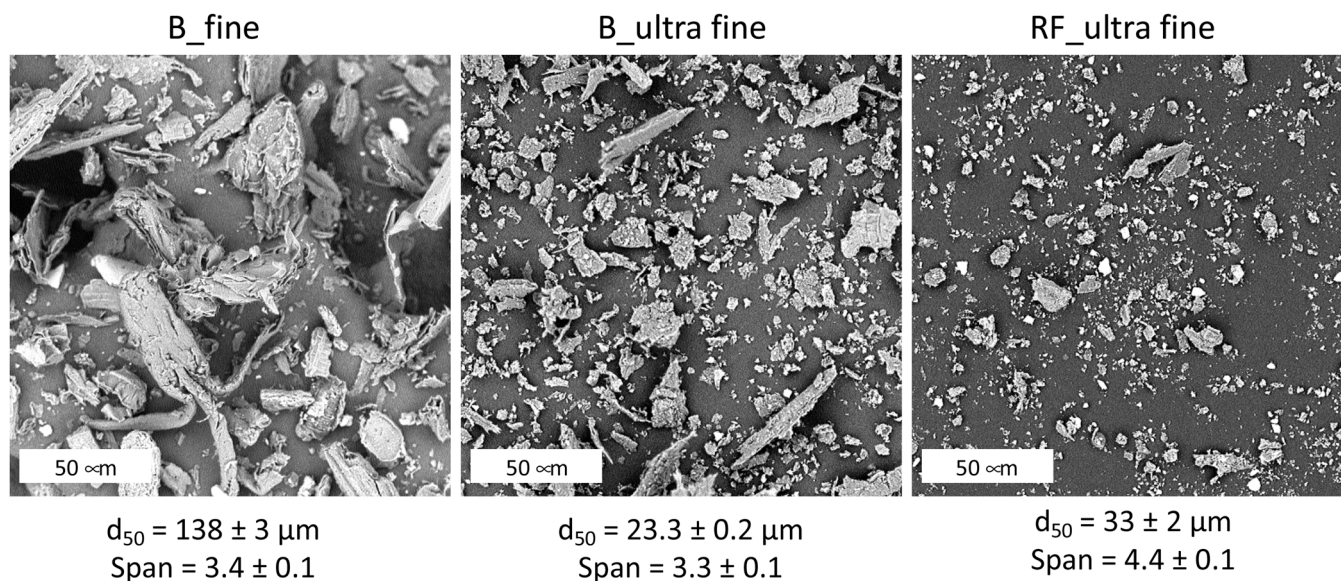


Fig. 2. SEM images and granulometric parameters of the three lignocellulosic fillers.

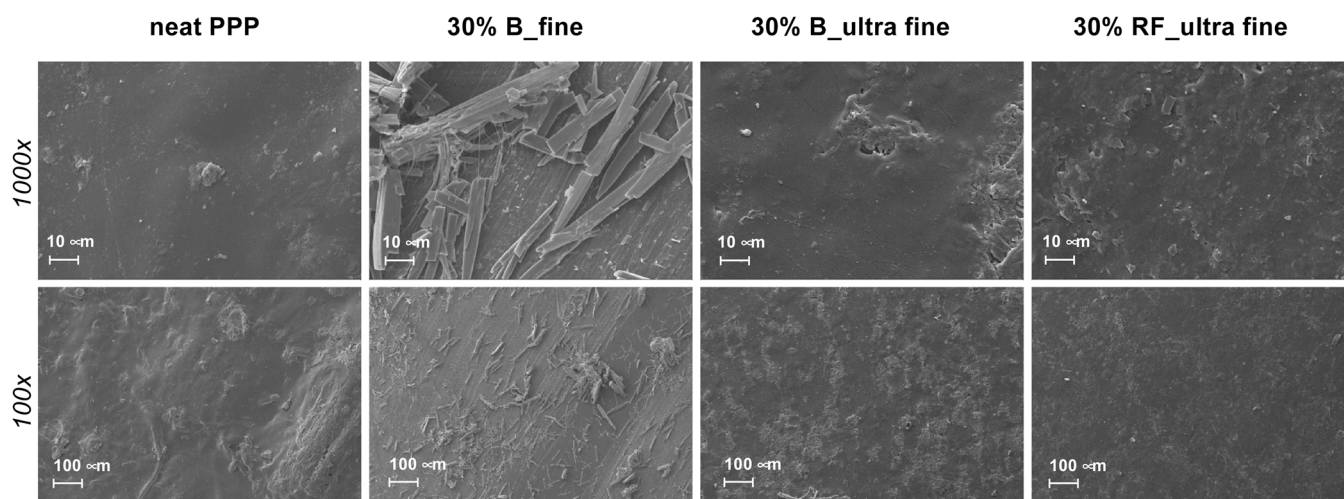


Fig. 3. SEM images of films made from neat porcine plasma protein (PPP) and with different lignocellulosic residue charges (30 wt%) of RF and B residues ground in an impact or ball mill (B_fine, B_ultra fine, RF_ultra fine).

Table 1

Colour parameters of porcine plasma protein/glycerol (1/1) films filled with different lignocellulosic particles (0, 5, 15, 30 wt%). Average values marked by different lower-case letters are statistically different ($p < 0.05$).

B_fine (wt%)	L	a*	b*	ΔE^*
0	32.47 ± 0.71 ^a	6.19 ± 0.44 ^a	4.23 ± 0.6 ^a	0.00
5	31.25 ± 0.35 ^a	4.61 ± 0.21 ^b	0.55 ± 0.05 ^b	4.18
15	28.83 ± 0.35 ^b	2.89 ± 0.04 ^c	-1.49 ± 0.05 ^c	7.54
30	30.70 ± 0.62 ^{a,b}	2.63 ± 0.07 ^c	-0.81 ± 0.19 ^c	6.41
B_ultra fine (wt%)	L	a*	b*	ΔE^*
0	32.47 ± 0.71 ^a	6.19 ± 0.44 ^a	4.23 ± 0.60 ^a	0.00
5	30.10 ± 0.08 ^a	4.09 ± 0.24 ^b	0.42 ± 0.17 ^b	4.95
15	30.36 ± 0.89 ^b	1.96 ± 0.12 ^c	-1.25 ± 0.04 ^c	7.23
30	31.11 ± 0.12 ^{a,b}	1.60 ± 0.08 ^c	-1.38 ± 0.18 ^c	7.37
RF_ultra fine (wt%)	L	a*	b*	ΔE^*
0	32.47 ± 0.71 ^a	6.19 ± 0.44 ^a	4.23 ± 0.60 ^a	0.00
5	31.78 ± 1.00 ^a	2.26 ± 0.14 ^a	-0.53 ± 0.18 ^b	6.21
15	24.7 ± 5.75 ^a	1.46 ± 0.02 ^b	-1.40 ± 0.04 ^{b,c}	10.70
30	30.80 ± 0.23 ^a	1.42 ± 0.00 ^b	-1.71 ± 0.03 ^c	7.80

62.6 MPa for the neat matrix up to 365.1 MPa for PPP filled with 30 wt% of B_fine). This phenomenon was progressively accentuated with increasing filler content. As regards the tensile strength, it remained globally constant up to 15 wt% of fillers (even if slight differences could be observed among samples), and then significantly increased for a filler content of 30 wt%. Mechanical properties of composites reinforced with fillers depend on different features of the fillers, like their volume content, aspect ratio, orientation or adhesion to the matrix (Saheb and Jog, 1999). The mechanical properties of composite materials have been expressed previously in terms of the moduli of their constituents through the rule of mixtures, considering their volume fractions (Montaño-Leyva et al., 2013). The increasing trend observed for Young's modulus of the composites might be attributed to rather good compatibility between the fillers and plasma protein. Previously, the establishment of interactions between a protein matrix and fillers has led to an anti-plasticizing effect produced by the filler, as observed in wheat gluten composites reinforced with fibres (Montaño-Leyva et al., 2013). Moreover, the lower deformability observed for the biocomposites might be explained by the reportedly low elongation of the fillers, which impedes the flow of the polymer (Paunonen, 2013).

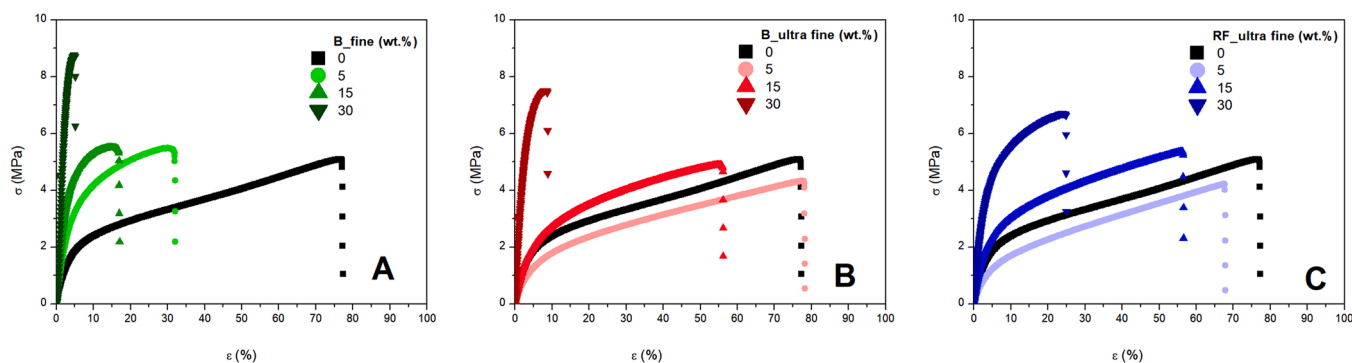


Fig. 4. Stress-deformation curves obtained through uniaxial tensile tests for composite films made from porcine plasma protein (PPP): glycerol (50:50) and different contents (0, 5, 15 and 30 wt%) of lignocellulosic fillers: (A) B_{fine}, (B) B_{ultra fine} and (C) RF_{ultra fine}.

Decreasing the size of the fillers from 138 μm (B_{fine}) to 23 μm (B_{ultra fine}) allowed to minimize the reduction of the strain at break with increasing filler content. Thus, at 15 wt%, the composite reinforced with B_{ultra fine} was three times more deformable than that reinforced with B_{fine}. This could be ascribed to a better dispersion state of the fillers with the polymer matrix, and/or to better interactions between the constituents, as already shown for PHBV/wheat straw composites (Berthet et al., 2015). However, the reduction of the size of the fillers resulted in less rigid (lower E) materials. Some authors have previously proven that the mechanical properties of poly (3-hydroxybutyrate-co-3-hydroxyvalerate) (PHBV) reinforced with filler are approximately linear functions of the reciprocal of the filler particle diameter, being independent of the nature of the filler (Alter, 1965). However, Avérous and Digabel have claimed that polybutylene adipate-co-terephthalate (PBAT) displayed higher mechanical properties by increasing the filler size (Avérous and Le Digabel, 2006). Also, this enhancement of the modulus and tensile strength with fillers of larger sizes has been reported for polypropylene/oil palm wood flour composites (Zaini et al., 1996). Thus, the effect of the lignocellulosic filler size on the mechanical properties is dependent on the system studied.

In the case of ultra-fine particles, the biomass type (B or RF) only had an effect for high filler content (30 wt%), with a larger increase of both Young's modulus and tensile strength, as well as a larger decrease of the strain at break for the branches-rich fraction than for the representative fraction. It seems thus that branches alone induce a greater strengthening that the whole representative fraction of the urban waste, in agreement with Viretto et al. (Viretto et al., 2021), who studied poly (3-hydroxybutyrate-co-3-hydroxyvalerate) (PHBV) plastic materials reinforced with different urban wastes. The poorer mechanical properties of the RF fraction were ascribed to the presence of grasses, which were demonstrated to govern the overall mechanical behaviour of the material even in low quantity (Viretto et al., 2021).

All biocomposites studied could be suitable for their application in packaging, as fillers promoted their rigidity and tensile strength. Thus, the filler content could be adjusted to obtain the desired mechanical features for specific purposes (Sánchez-Safont et al., 2018).

3.4. Dynamic mechanical thermal analysis (DMTA)

Frequency sweep tests were performed at 25 $^{\circ}\text{C}$ for all biocomposites studied, obtaining the corresponding mechanical spectra (i.e., elastic modulus, E' , and viscous modulus, E'' , versus frequency). From these mechanical spectra, the average values of E' and E'' at 1 Hz ($E'_{1\text{ Hz}}$, $E''_{1\text{ Hz}}$) were estimated (Fig. 6). The evolution of E' with the lignocellulosic filler content was quite similar to that reported in the previous section for Young's modulus, and an increase in the amount of urban waste generally promoted a rise in the values of E' . Thus, $E'_{1\text{ Hz}}$ increased from 340 for the neat matrix to 830 MPa for the composite

reinforced with 30 wt% B_{fine}, as a consequence of the reinforcement of the structure. However, when lower amounts of filler were introduced in the sample (5 wt%), the viscoelastic properties did not reveal any reinforcement, even finding a significant softening of the material when employing the B_{fine} fraction. On the other hand, it should be highlighted that biocomposites including branches from urban wastes of greater particle size (B_{fine}) displayed significantly poorer viscoelastic properties at 5 or even 15 wt% contents than the neat matrix. The replacement of that filler by another of the same nature but much smaller sizes (B_{ultra fine}) produced an important increase in E' , although those differences disappeared at the greatest content studied (30 wt%). The commented evolution was affected by the biomass type, and the use of RF_{ultra fine} as lignocellulosic filler produced a much milder increase of E' at the highest level content. Thus, $E'_{1\text{ Hz}}$ for RF_{ultra fine} composites at 30 wt% increased just 1.3 times when compared to the neat matrix, and B_{fine} and B_{ultra fine} composites displayed an increase of 2.7 and 0.5 times, respectively. This is again coherent with the evolution observed for Young's modulus.

Fig. 7 shows the evolution followed by the E' and E'' (Fig. 7A) and loss tangent ($\tan \delta$) (Fig. 7B) when plasma-based composites containing 30 wt% of lignocellulosic fillers (B_{fine}, B_{ultra fine}, RF_{ultra fine}) were heated from -80 – 120 $^{\circ}\text{C}$. A control system not containing any filler was also included. All samples showed a decrease in both viscoelastic moduli along the whole temperature ramp test, a characteristic behaviour of thermoplastic materials (Álvarez-Castillo et al., 2020b). This thermoplastic behaviour has already been observed for other protein systems, either animal or vegetable ones (Álvarez-Castillo et al., 2021b, 2019; Delgado et al., 2018; Fernández-Espada et al., 2016; Perez-Puyana et al., 2016). No thermoset behaviour was observed when heating since the majority of thermal crosslinking was already produced during the compression moulding stage at 150 $^{\circ}\text{C}$ (Álvarez-Castillo et al., 2019). Different E' and $\tan \delta$ values were detected when different lignocellulosic fractions (i.e., different composition and/or particle size) were used within the composite formulation. When employing branches, regardless of the particle size (B_{fine} or B_{ultra fine}), both viscoelastic moduli were much higher during the whole DMTA test when compared to the control system. Thus, particle size did not exert a great influence on the thermo-rheological response of these materials, even if higher Young's moduli were detected for the impact mill sample (Fig. 5). When assessing the effect of the nature of the biomass, it should be noticed that the presence of a representative fraction as lignocellulosic filler ground with a ball mill (RF_{ultra fine}) did not affect significantly the thermo-rheological behaviour compared to the neat sample, as the response of the control system (0 wt%) and RF_{ultra fine} overlapped during most of the DMTA test. However, the decay in E'' from 20 $^{\circ}\text{C}$ on was more profound in the absence of the filler, evidencing greater thermal stability when reinforced by RF. Even if both B_{ultra fine} and RF_{ultra fine} possessed almost the same particle size (~ 20 – 30 μm), branches imparted a greater reinforcement and thermal stability than

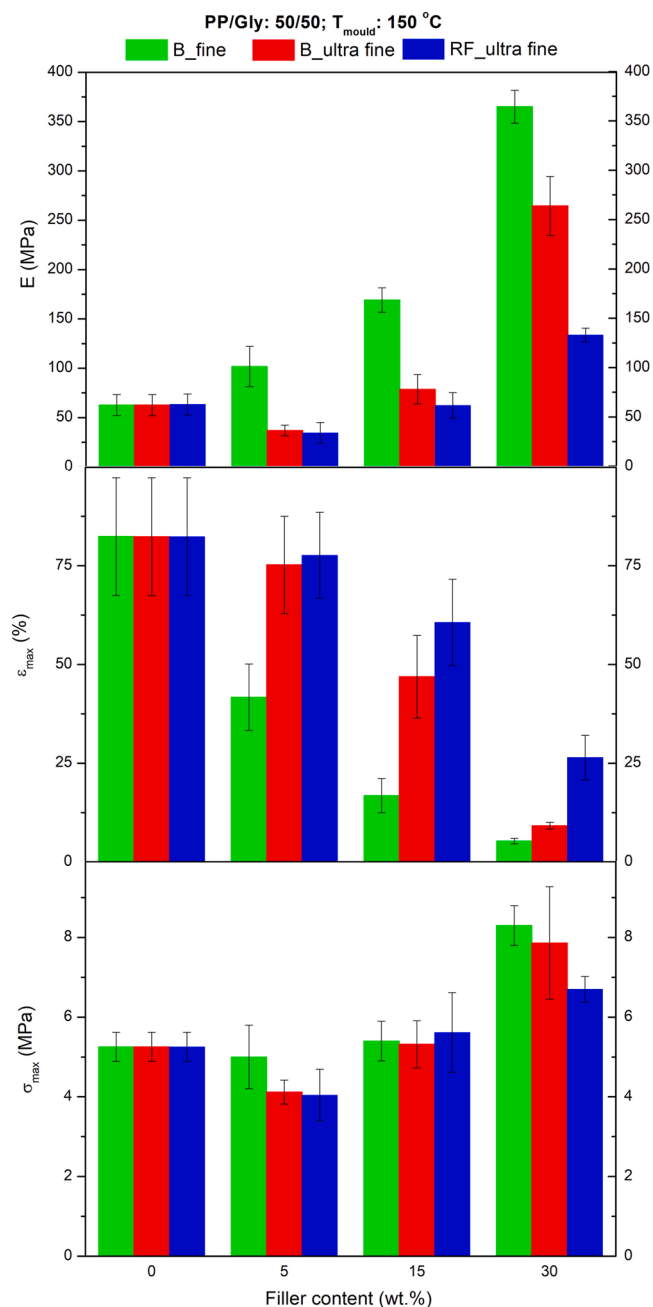


Fig. 5. Main mechanical parameters (Young's modulus (E); strain at break (ϵ_{max}); and tensile strength (σ_{max})) obtained through uniaxial tensile tests for films made from porcine plasma protein:glycerol (50:50) and with different lignocellulosic residue charges (0, 5, 15, 30 wt%) of branches (B_fine and B_ultra fine) and a representative fraction (RF_ultra fine) residues.

the complete urban waste (including not only branches but also leaves or grass). These results agree with the evolution observed for the mechanical properties.

Regarding the loss tangent, $\tan \delta$, the existence of two different peaks can be clearly distinguished: there is a first one placed at lower temperatures, with a maximum for all systems located at approximately -57°C . This thermal transition has been associated either with a β -relaxation phenomenon or the presence of a glycerol-rich region in the composite, which is due to the presence of the plasticizer (Christoph et al., 2000). This T_g at -57°C was higher than the value reported for pure glycerol (-93°C), which might be explained on basis of the existence of certain plasma protein domains that were miscible with glycerol (Cherian et al.,

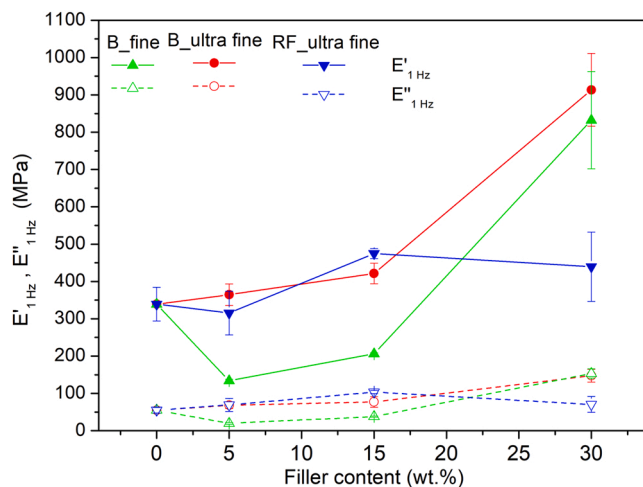


Fig. 6. Impact of filler content of elastic moduli values (E' and E'') of PPP:glycerol (50:50) films filled with B_fine, B_ultra fine and RF_ultra fine.

1995; Ghanbarzadeh and Oromiehi, 2008). A second peak at greater temperatures can be associated with a protein-rich region within the material, which in the case of the control system overlapped with the first one. This overlap of these $\tan \delta$ peaks has been reported as a sign of good compatibility between the ingredients (i.e., plasticizer and protein). However, those peaks were separated to a greater extent in the biocomposites with branches, as they displayed an easily distinguishable second peak displaced onto higher temperatures ($60\text{--}70^\circ\text{C}$) when compared to the control system. The presence of the filler seems to impart an antiplasticizer effect, independently of the nature of the lignocellulosic urban waste. The greater separation between those two peaks found for branches fillers, either B_fine or B_ultra fine, seems to reveal a greater degree of incompatibility among the plasticizer and the PPP in the presence of the filler based exclusively on branches, indicating a presumable higher antiplasticizer effect. Antiplasticization results from strong interactions between glycerol and the polymer that cause loss of mobility within the macromolecular chains (Singh and Gupta, 2016). Biocomposite samples also showed some degree of exudation of glycerol after being stored for 1 week. Remarkably, the temperature at which the second peak was detected approximately matched the gelation temperature reported for plasma protein (Álvarez-Castillo et al., 2020a, 2019).

3.5. Water uptake

No statistically significant ($p < 0.05$) difference was observed neither in WUC for the plasma-based composites filled with B_fine when compared to the control system, observing an average value of 114% (Table 2). The use of a branch fraction with smaller sizes (B_ultra fine) did not alter remarkably the values, except at 15 wt%, when a tendency for higher values was detected. When biomass including a representative fraction of the urban biowastes, RF_ultrafine, was used, a tendency upwards evolution in WUC was observed as RF_ultrafine content increased in the biocomposite, possibly due to the greater hydrophilicity of the rest of the compounds in the biowaste used as filler. In any case, all samples could retain between one and two times their weight in water.

When observing the soluble matter loss (SML), it can be seen that the greater the amount of glycerol introduced in the sample, the greater the material lost during the immersion. It should be pointed out that the glycerol content was lower as the amount of lignocellulosic filler was higher. Thus, it seems that the plasticizer was the main part lost during the immersion stage from the composite, which is in agreement with previous studies that reported that the hydrophilic character of glycerol makes it quite soluble in the aqueous medium (Álvarez-Castillo et al.,

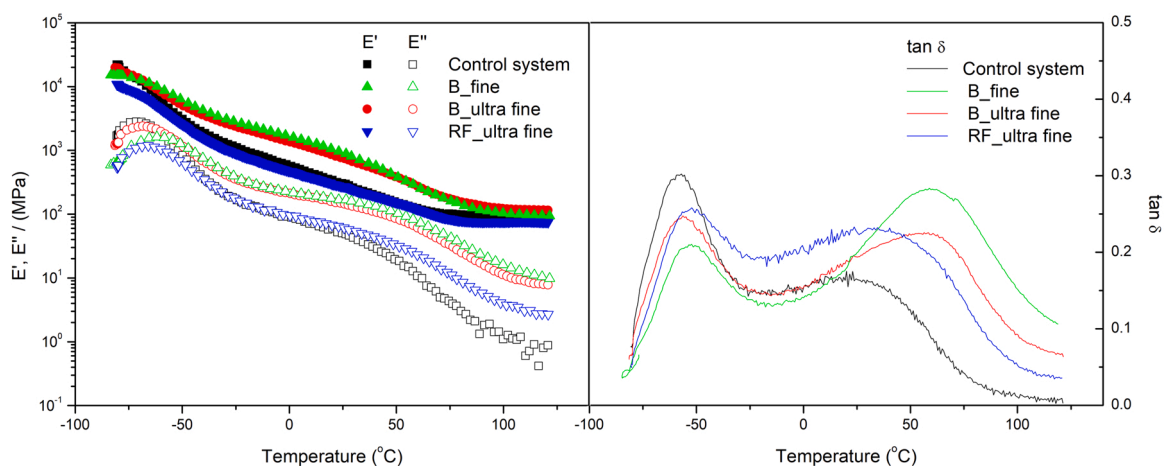


Fig. 7. Rheological parameters (E' , E'' (left) and $\tan \delta$ (right)) from DMTA tests in bending mode at a constant frequency (1 Hz) of films made from porcine plasma protein:glycerol (50:50) and with different lignocellulosic residue charges (30 wt%) of RF and branches residues ground in an impact or ball mill (B_fine, B_ultra fine, RF_ultra fine).

Table 2

		Water uptake (%)			Soluble matter loss (%)		
		B_fine	B_ultra fine	RF_ultrafine	B_fine	B_ultra fine	RF_ultrafine
% filler	0	117 ± 12 ^{a,b}			53.2 ± 0.6 ^a		
	5	122 ± 20 ^a	105 ± 7 ^a	112 ± 7 ^a	55.5 ± 1.5 ^a	52.2 ± 0.4 ^a	53.2 ± 0.8 ^a
	15	117 ± 10 ^a	173 ± 18 ^b	138 ± 31 ^{a,b}	48.4 ± 1.1 ^b	47.0 ± 0.8 ^b	47.8 ± 0.3 ^b
	30	99 ± 5 ^a	90 ± 5 ^a	183 ± 33 ^b	39.6 ± 0.6 ^c	39.3 ± 0.6 ^c	41.0 ± 3.1 ^c

2021a). Thus, independently of the urban biowaste used (B_fine, B_ultra fine, RF_ultra fine) as filler in the composite, the amount of soluble matter loss decreased as a higher amount of the filler was introduced in the formulation.

3.6. Water Vapour and oxygen Permeability

In general terms, proteins are macromolecules with an important hydrophilic character, usually showing poor water vapour barrier properties while acting as a good barrier for non-polar gases such as O₂ and CO₂ (Guilbert et al., 1995).

Water vapour permeability (WVP) tests determine the resistance of a material to be penetrated by water vapour per time and area of the material. Fig. 8 illustrates the WVP values obtained for PPP control films ($0.85 \pm 0.05 \times 10^{-10} \text{ mol}\cdot\text{m}^{-1}\cdot\text{s}^{-1}\cdot\text{Pa}^{-1}$) and of composites with different fractions of lignocellulosic biowaste (B_fine, B_ultra fine, RF_ultra fine)

at different concentration levels. From these results, it could be perceived that the introduction of any type of urban waste as a filler (RF or branches) in the composition does not influence significantly WVP if the concentration was lower than 30 wt%. This would prove that intermolecular interactions between lignocellulosic biowastes, plasma protein and the plasticizer that have taken place during the processing of the plastic materials did not have a significant influence on the WVP at the above-commented concentration levels (Cho and Rhee, 2004). Otherwise, when the amount of filler used was 30 wt%, a similar apparent increase (ca. 20%) in the WVP (up to $1.0\text{--}1.1 \times 10^{-10} \text{ mol}\cdot\text{m}^{-1}\cdot\text{s}^{-1}\cdot\text{Pa}^{-1}$) was detected for all the fillers. Thus, from these results it can be concluded that the presence of the studied lignocellulosic biowastes at high concentrations (30 wt%) in the composites increases the WVP, resulting in lower barrier materials to water vapour.

Regarding the Oxygen permeability (OP), Fig. 6 shows that the presence of the urban biowastes fillers on the composites led to a

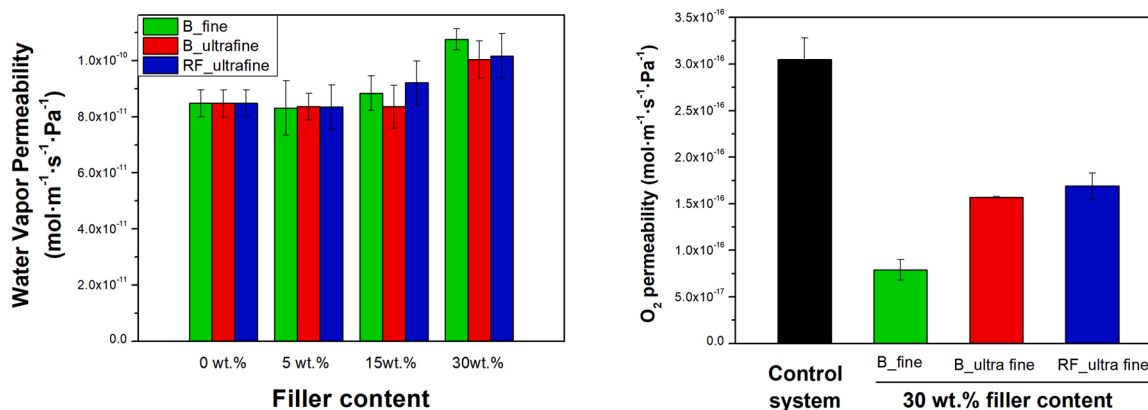


Fig. 8. Water Vapour (left) and Oxygen (right) Permeability of biocomposite films made from porcine plasma protein:glycerol (50:50) including different lignocellulosic biowastes at different concentration levels (0, 5, 15, 30 wt%).

decrease in their oxygen permeability ($1.6\text{--}1.7 \times 10^{-16} \text{ mol}\cdot\text{m}^{-1}\cdot\text{s}^{-1}\cdot\text{Pa}^{-1}$ for RFUltra fine and BUltra fine) when compared to the control film ($3.0 \times 10^{-16} \text{ mol}\cdot\text{m}^{-1}\cdot\text{s}^{-1}\cdot\text{Pa}^{-1}$). The higher OP showed by the control system might be justified by the higher amount of plasticizer used in its composition. McHugh (Sukhija et al., 2016) determined that the amount of glycerol used as a plasticizer for the film formation would influence the OP of the material, determining that a higher quantity of plasticizer would relax the film structure, forming a more porous structure that allows easier penetration of oxygen through the film. Additionally, the use of an impact mill (B_{fine}) resulted in a bigger decrease in OP ($0.8 \times 10^{-16} \text{ mol}\cdot\text{m}^{-1}\cdot\text{s}^{-1}\cdot\text{Pa}^{-1}$), which could be motivated by the differences in the granulometry of the particles. For all samples, values are in the same order of magnitude as synthetic polymers, such as low-density polyethylene ($1\text{--}2 \times 10^{-15} \text{ mol}\cdot\text{m}^{-1}\cdot\text{s}^{-1}\cdot\text{Pa}^{-1}$) (Durmuş et al., 2007; Matar et al., 2018; Motedayen et al., 2019) and polypropylene ($0.1\text{--}5.0 \times 10^{-16} \text{ mol}\cdot\text{m}^{-1}\cdot\text{s}^{-1}\cdot\text{Pa}^{-1}$) (Jung et al., 2021; Klepac et al., 2014), as well as bio-based polymers such as polylactic acid (PLA) (1×10^{-16} and $1 \times 10^{-14} \text{ mol}\cdot\text{m}^{-1}\cdot\text{s}^{-1}\cdot\text{Pa}^{-1}$) (Lehermeier et al., 2001; Mahmoodi et al., 2019; Palai et al., 2019).

In conclusion, the inclusion of 30% fillers can slightly increase WVP (18–29%) while decreasing OP (43–73%), which might be interesting for oxygen-sensitive products.

4. Concluding remarks

The present work focused on the development of composites based on porcine plasma protein as matrix and lignocellulosic particles produced from urban parks and gardens' green waste as fillers. As the amount of lignocellulosic biowaste increased, the colour of the samples darkened noticeably and an increase in Young's modulus and tensile strength was observed. Regarding the type of filler used, the branches-rich fraction imparted the greatest reinforcement as compared to a representative fraction of the whole urban biowaste, when employing similar particle sizes. Also, higher Young's modulus and tensile strength were detected when employing larger particle sizes of the same type of filler, pointing out the importance of the grinding stage. When studying the thermomechanical properties of those composites, an antiplasticizing effect exerted by the biowaste when introduced as filler was revealed by the evolution of loss tangent. Thus, peaks corresponding to the glycerol-rich and protein-rich regions only overlapped when there was no filler included in the composite, despite including a higher glycerol content. The antiplasticizing effect was seemingly higher when branches instead of the whole biowaste were used as fillers.

The addition of fillers did not cause any significant effect on the water uptake of the protein-based composites, independently of the nature and content of the filler used. Water vapour permeability only increased if the content of lignocellulosic biowaste in the formulation of the sample was 30 wt%, notwithstanding the fraction used. Also, oxygen permeability decreased when a lignocellulosic biowaste was included, especially if it was ground with an impact grinder.

CRediT authorship contribution statement

All of the authors listed on the manuscript made a substantial contribution, quality for authorship, and no authors have been omitted. **Carlos Bengoechea:** Investigation, Conceptualization, Methodology, Software, Writing – review & editing, Funding acquisition; **Ana Paula Batista:** Investigation, Data curation, Writing – original draught preparation; **Estefanía Álvarez-Castillo:** Writing review & editing; **Antonio Guerrero:** Supervision, Funding acquisition; **Nathalie Gontard:** Supervision, Funding acquisition.; **Helene Angellier-Coussy:** Project administration, Resources, Writing – review & editing.

Declaration of Competing Interest

The authors declare that they have no known competing financial

interests or personal relationships that could have appeared to influence the work reported in this paper.

Data availability

Data will be made available on request.

Acknowledgements

The authors acknowledge the project PID2021–124294OB-C21 funded by MCIN/AEI/10.13039/501100011033/ and by “ERDF A way of making Europe” which supported this study. The authors also would like to the Spanish Ministerio de Ciencia, Innovación y Universidades for the grant PRX18/00333 (Salvador de Madariaga programme) awarded to C. Bengoechea, and Ministerio de Universidades for the PhD grant PRE2019–089815 awarded to E. Álvarez-Castillo. The urban parks and gardens' green waste were collected in the frame of the RESURBIS project, which was supported by the European commission through the Horizon 2020 work program for research & innovation under the grant agreement 730349. The authors thank Amandine Viretto for SEM observations of lignocellulosic fillers.

References

- Abascal, N.C., Regan, L., 2018. The past present and future of protein-based materials. *R. Soc. Open Biol.* 8, 180113.
- Alter, H., 1965. Filler particle size and mechanical properties of polymers. *J. Appl. Polym. Sci.* 9, 1525–1531. <https://doi.org/10.1002/app.1965.070090427>.
- Álvarez, C., Rendueles, M., Díaz, M., 2012. Production of porcine hemoglobin peptides at moderate temperature and medium pressure under a nitrogen stream. functional and antioxidant properties. *J. Agric. Food Chem.* 60, 5636–5643. <https://doi.org/10.1021/jf300400k>.
- Álvarez-Castillo, E., Bengoechea, C., Rodríguez, N., Guerrero, A., 2019. Development of green superabsorbent materials from a by-product of the meat industry. *J. Clean. Prod.* 223, 651–661. <https://doi.org/10.1016/j.jclepro.2019.03.055>.
- Álvarez-Castillo, E., Bengoechea, C., Guerrero, A., 2020a. Effect of pH on the properties of porcine plasma-based superabsorbent materials. *Polym. Test.* 85, 106453 <https://doi.org/10.1016/j.polymertesting.2020.106453>.
- Álvarez-Castillo, E., Bengoechea, C., Guerrero, A., 2020b. Composites from by-products of the food industry for the development of superabsorbent biomaterials. *Food Bioprod. Process.* 119, 296–305. <https://doi.org/10.1016/j.fbp.2019.11.009>.
- Álvarez-Castillo, E., Oliveira, S.S., Bengoechea, C., Sousa, I., Raymundo, A., Guerrero, A., 2020c. A rheological approach to 3d printing of plasma protein based doughs. *J. Food Eng.* 288, 110255 <https://doi.org/10.1016/j.jfoodeng.2020.110255>.
- Álvarez-Castillo, E., Bengoechea, C., Guerrero, A., 2021a. Strengthening of porcine plasma protein superabsorbent materials through a solubilization-freeze-drying process. *Polymers* 13. <https://doi.org/10.3390/polym13050772>.
- Álvarez-Castillo, E., Caballero, G., Guerrero, A., Bengoechea, C., 2021b. Effect of formulation and pressure on injection moulded soy protein-based plastics. *J. Polym. Environ.* <https://doi.org/10.1007/s10924-021-02082-w>.
- Ashter, S.A., 2016. Processing Biodegradable Polymers. In: Ashter, S.A.B.T.-I., B.E. (Eds.), *Introduction to Bioplastics Engineering*. Elsevier, Oxford, pp. 179–209. <https://doi.org/10.1016/B978-0-323-39396-6.00007-5>.
- ASTM-E96/E96M, 2016. Standard Test Methods for Water Vapor Transmission of materials, West Conshohocken 14p.
- Avérous, L., Le Digabel, F., 2006. Properties of biocomposites based on lignocellulosic fillers. *Carbohydr. Polym.* 66, 480–493. <https://doi.org/10.1016/j.carbpol.2006.04.004>.
- Bah, C.S.F., Bekhit, A.E.-D.A., Carne, A., McConnell, M.A., 2013. Slaughterhouse blood: an emerging source of bioactive compounds. *Compr. Rev. Food Sci. Food Saf.* 12, 314–331. <https://doi.org/10.1111/1541-4337.12013>.
- Belyaeva, O.N., Haynes, R.J., 2009. Chemical microbial and physical properties of manufactured soils produced by co-composting municipal green waste with coal fly ash. *Bioresour. Technol.* 100, 5203–5209. <https://doi.org/10.1016/j.biortech.2009.05.032>.
- Berthet, M.-A., Angellier-Coussy, H., Chea, V., Guillard, V., Gastaldi, E., Gontard, N., 2015. Sustainable food packaging: valorizing wheat straw fibres for tuning PHBV-based composites properties. *Compos. Part A Appl. Sci. Manuf.* 72, 139–147. <https://doi.org/10.1016/j.compositesa.2015.02.006>.
- Bustamante, M.A., Ceglie, F.G., Aly, A., Mihreteab, H.T., Ciaccia, C., Tittarelli, F., 2016. Phosphorus availability from rock phosphate: Combined effect of green waste composting and sulfur addition. *J. Environ. Manag.* 182, 557–563. <https://doi.org/10.1016/j.jenvman.2016.08.016>.
- Cherian, G., Gennadios, a, Weller, C., Chinachoti, P., 1995. Thermomechanical behavior of wheat gluten films: effect of sucrose glycerin and sorbitol. *Cereal Chem.* 72, 1–6.
- Cho, S.Y., Rhee, C., 2004. Mechanical properties and water vapor permeability of edible films made from fractionated soy proteins with ultrafiltration. *LWT Food Sci. Technol.* 37, 833–839. <https://doi.org/10.1016/j.lwt.2004.03.009>.

- Christoph, R., Schmidt, B., Steinberner, U., Dilla, W., Karinen, R., 2000. Glycerol. Ullmann's Encycl. Ind. Chem.
- Cuadri, A.A.A., Romero, A., Bengochea, C., Guerrero, A., 2017. Natural superabsorbent plastic materials based on a functionalized soy protein. *Polym. Test.* 58, 126–134. <https://doi.org/10.1016/j.polymertesting.2016.12.024>.
- David, G., Vannini, M., Sisti, L., Marchese, P., Celli, A., Gontard, N., Angellier-Coussy, H., 2020. Eco-conversion of two winery lignocellulosic wastes into fillers for biocomposites: vine shoots and wine pomaces. *Polymers* 12, 1530. <https://doi.org/10.3390/polym12071530>.
- Dávila, E., Parés, D., Cuvelier, G., Relkin, P., 2007. Heat-induced gelation of porcine blood plasma proteins as affected by pH. *Meat Sci.* 76, 216–225. <https://doi.org/10.1016/j.meatsci.2006.11.002>.
- Delgado, M., Felix, M., Bengochea, C., 2018. Development of bioplastic materials: from rapeseed oil industry by products to added-value biodegradable biocomposite materials. *Ind. Crops Prod.* 125, 401–407.
- Durmuş, A., Woo, M., Kaşgöz, A., Macosko, C.W., Tspatsis, M., 2007. Intercalated linear low density polyethylene (LLDPE)/clay nanocomposites prepared with oxidized polyethylene as a new type compatibilizer: structural mechanical and barrier properties. *Eur. Polym. J.* 43, 3737–3749. <https://doi.org/10.1016/j.eurpolymj.2007.06.019>.
- Eades, P., Kusch-Brandt, S., Heaven, S., Banks, C.J., 2020. Estimating the generation of garden waste in England and the differences between rural and urban areas. *Resources* 9. <https://doi.org/10.3390/resources9010008>.
- Elzoghby, A.O., Samy, W.M., Elgindy, N.A., 2012. Protein-based nanocarriers as promising drug and gene delivery systems. *J. Control. Release* 161, 38–49. <https://doi.org/10.1016/j.jconrel.2012.04.036>.
- Fernández-Espada, L., Bengochea, C., Cordobés, F., Guerrero, A., 2016. Protein/glycerol blends and injection-molded bioplastic matrices: soybean versus egg albumen. *J. Appl. Polym. Sci.* <https://doi.org/10.1002/app.42980>.
- Francou, C., Linères, M., Derenne, S., Villio-Poitrenaud, M., Le, Houot, S., 2008. Influence of green waste biowaste and paper-cardboard initial ratios on organic matter transformations during composting. *Bioresour. Technol.* 99, 8926–8934. <https://doi.org/10.1016/j.biortech.2008.04.071>.
- Ghanbarzadeh, B., Oromiehi, A.R., 2008. Studies on glass transition temperature of mono and bilayer protein films plasticized by glycerol and olive oil. *J. Appl. Polym. Sci.* 109, 2848–2854. <https://doi.org/10.1002/app.28289>.
- Guilbert, S., Gontard, N., Cuq, B., 1995. Technology and applications of edible protective films. *Packag. Technol. Sci.* <https://doi.org/10.1002/pts.2770080607>.
- Haynes, R.J., Belyaeva, O.N., Zhou, Y.-F., 2015. Particle size fractionation as a method for characterizing the nutrient content of municipal green waste used for composting. *Waste Manag.* 35, 48–54. <https://doi.org/10.1016/j.wasman.2014.10.002>.
- Hurtado, S., Dagà, I., Espigulé, E., Parés, D., Saguer, E., Toldrà, M., Carretero, C., 2011. Use of porcine blood plasma in “phosphate-free frankfurters”. *Procedia Food Sci.* 1, 477–482. <https://doi.org/10.1016/j.profoo.2011.09.073>.
- Hurtado, S., Saguer, E., Toldrà, M., Parés, D., Carretero, C., 2012. Porcine plasma as polyphosphate and caseinate replacer in frankfurters. *Meat Sci.* 90, 624–628. <https://doi.org/10.1016/j.meatsci.2011.10.004>.
- Ibbett, R., Gaddipati, S., Tucker, G., 2019. In-situ studies of hydrothermal reactions of lignocellulosic biomass using high-pressure differential scanning calorimetry. *Biomass Bioenergy* 121, 48–55. <https://doi.org/10.1016/j.biombioe.2018.12.006>.
- Jiménez, M.Á., González-Muñoz, R., 2019. Peptides in biology and biomedicine: walking towards the future. *Arch. Biochem. Biophys.* 665, 20–22. <https://doi.org/10.1016/j.abb.2019.02.010>.
- Jiménez-Rosado, M., Pérez-Puyana, V., Cordobés, F., Romero, A., Guerrero, A., 2018. Development of soy protein-based matrices containing zinc as micronutrient for horticulture. *Ind. Crops Prod.* 121, 345–351. <https://doi.org/10.1016/j.indcrop.2018.05.039>.
- Jung, B.-N., Jung, H.-W., Kang, D.-H., Kim, G.-H., Shim, J.-K., 2021. A Study on the oxygen permeability behavior of nanoclay in a polypropylene/nanoclay nanocomposite by biaxial stretching. *Polymers* 13. <https://doi.org/10.3390/polym13162760>.
- Klepac, D., Šćetar, M., Baranović, G., Galić, K., Valić, S., 2014. Influence of high doses γ -irradiation on oxygen permeability of linear low-density polyethylene and cast polypropylene films. *Radiat. Phys. Chem.* 97, 304–312. <https://doi.org/10.1016/j.radphyschem.2013.12.005>.
- Kranert, M., Gottschall, R., Bruns, C., Hafner, G., 2010. Energy or compost from green waste? - A CO₂ - based assessment. *Waste Manag.* 30, 697–701. <https://doi.org/10.1016/j.wasman.2009.09.046>.
- Kriegel, C., Arrechi, A., Kit, K., McClements, D.J., Weiss, J., 2008. Fabrication functionalization and application of electrospun biopolymer nanofibers. *Crit. Rev. Food Sci. Nutr.* <https://doi.org/10.1080/10408390802241325>.
- Kumar, M., Ou, Y.-L., Lin, J.-G., 2010. Co-composting of green waste and food waste at low C/N ratio. *Waste Manag.* 30, 602–609. <https://doi.org/10.1016/j.wasman.2009.11.023>.
- Lehermeier, H.J., Dorgan, J.R., Way, J.D., 2001. Gas permeation properties of poly(lactic acid). *J. Memb. Sci.* 190, 243–251. [https://doi.org/10.1016/S0376-7388\(01\)00446-X](https://doi.org/10.1016/S0376-7388(01)00446-X).
- López-Castejón, M.L., Bengochea, C., García-Morales, M., Martínez, I., 2016. Influence of tragacanth gum in egg white based bioplastics: thermomechanical and water uptake properties. *Carbohydr. Polym.* 152, 62–69. <https://doi.org/10.1016/j.carbpol.2016.06.041>.
- Lynch, S.A., Mullen, A.M., O'Neill, E.E., García, C.Á., 2017. Harnessing the potential of blood proteins as functional ingredients: a review of the state of the art in blood processing. *Compr. Rev. Food Sci. Food Saf.* 16, 330–344. <https://doi.org/10.1111/1541-4337.12254>.
- MacFarlane, D.W., 2009. Potential availability of urban wood biomass in michigan: implications for energy production carbon sequestration and sustainable forest management in the U.S.A. *Biomass Bioenergy* 33, 628–634. <https://doi.org/10.1016/j.biombioe.2008.10.004>.
- Mahmoodi, A., Ghodrati, S., Khorasani, M., 2019. High-strength low-permeable and light-protective nanocomposite films based on a hybrid nanopigment and biodegradable pla for food packaging applications. *ACS Omega* 4, 14947–14954. <https://doi.org/10.1021/acsomega.9b01731>.
- Matar, C., Gaucel, S., Gontard, N., Guilbert, S., Guillard, V., 2018. Predicting shelf life gain of fresh strawberries 'Charlotte cv' in modified atmosphere packaging. *Postharvest Biol. Technol.* 142, 28–38. <https://doi.org/10.1016/j.postharvbio.2018.03.002>.
- Mohanty, A.K., Tummala, P., Liu, W., Misra, M., Mulukutla, P.V., Drzal, L.T., 2005. Injection molded biocomposites from soy protein based bioplastic and short industrial hemp fiber. *J. Polym. Environ.* 13, 279–285. <https://doi.org/10.1007/s10924-005-4762-6>.
- Montaño-Leyva, B., da Silva, G.G.D., Gastaldi, E., Torres-Chávez, P., Gontard, N., Angellier-Coussy, H., 2013. Biocomposites from wheat proteins and fibers: structure/mechanical properties relationships. *Ind. Crops Prod.* 43, 545–555. <https://doi.org/10.1016/j.indcrop.2012.07.065>.
- Motedayen, A.A., Rezaeigolestani, M., Guillaume, C., Guillard, V., Gontard, N., 2019. Gas barrier enhancement of uncharged apolar polymeric films by self-assembling stratified nano-composite films. *RSC Adv.* 9, 10938–10947.
- Nechita, P., Dobrin, E., Ciolacu, F., Bobu, E., 2010. the biodegradability and mechanical strength of. *BioResources* 5, 1102–1113.
- Nuthong, P., Benjakul, S., Prodpran, T., 2009a. Characterization of porcine plasma protein-based films as affected by pretreatment and cross-linking agents. *Int. J. Biol. Macromol.* 44, 143–148. <https://doi.org/10.1016/j.ijbiomac.2008.11.006>.
- Nuthong, P., Benjakul, S., Prodpran, T., 2009b. Effect of phenolic compounds on the properties of porcine plasma protein-based film. *Food Hydrocoll.* 23, 736–741. <https://doi.org/10.1016/j.foodhyd.2008.08.003>.
- Nuthong, P., Benjakul, S., Prodpran, T., 2009c. Effect of some factors and pretreatment on the properties of porcine plasma protein-based films. *LWT Food Sci. Technol.* 42, 1545–1552. <https://doi.org/10.1016/j.lwt.2009.05.003>.
- Palai, B., Biswal, M., Mohanty, S., Nayak, S.K., 2019. In situ reactive compatibilization of polylactic acid (PLA) and thermoplastic starch (TPS) blends; synthesis and evaluation of extrusion blown films thereof. *Ind. Crops Prod.* 141, 111748. <https://doi.org/10.1016/j.indcrop.2019.11.1748>.
- Paunonen, S., 2013. Strength and barrier enhancements of cellophane and cellulose derivative films: a review. *BioResources* 8, 3098–3121. <https://doi.org/10.15376/biores.8.2.3098-3121>.
- Perez-Puyana, V., Felix, M., Romero, A., Guerrero, A., Perez, V., Felix, M., Romero, A., Guerrero, A., Perez-Puyana, V., Felix, M., Romero, A., Guerrero, A., 2016. Characterization of pea protein-based bioplastics processed by injection moulding. *Food Bioprod. Process.* 97, 100–108. <https://doi.org/10.1016/j.fbp.2015.12.004>.
- Peters, T., 1975. 3 - Serum Albumin, in: PUTNAM, F.W.B.T.-T.P.P. (Second E. (Ed.), Academic Press, pp. 133–181. <https://doi.org/https://doi.org/10.1016/B978-0-12-568401-9.50010-4>.
- Piot, J.M., Guillochon, D., Thomas, D., 1986. Preparation of decolorized peptides from slaughter-house blood. *MIRCEN J. Appl. Microbiol. Biotechnol.* 2, 359–364.
- Pratibha, Saha, Hariprasad, P. S., 2022. Paddy straw-based biodegradable horticultural pots: an integrated greener approach to reduce plastic waste valorize paddy straw and improve plant health. *J. Clean. Prod.* 337, 130588. <https://doi.org/10.1016/j.jclepro.2022.130588>.
- Raeker, M.Ö.M., Johnson, L.A.A., 1995. Thermal and functional properties of bovine blood plasma and egg white proteins. *J. Food Sci.* 60, 685–690. <https://doi.org/10.1111/j.1365-2621.1995.tb06206.x>.
- Razzaq, H.A.A., Pezzuto, M., Santagata, G., Silvestre, C., Cimmino, S., Larsen, N., Duraccio, D., 2016. Barley β -glucan-protein based bioplastic film with enhanced physicochemical properties for packaging. *Food Hydrocoll.* 58, 276–283. <https://doi.org/10.1016/j.foodhyd.2016.03.003>.
- Reyes-Torres, M., Oviedo-Ocaña, E.R., Dominguez, I., Komilis, D., Sánchez, A., 2018. A systematic review on the composting of green waste: feedstock quality and optimization strategies. *Waste Manag.* 77, 486–499. <https://doi.org/10.1016/j.wasman.2018.04.037>.
- Rhim, J.W., Park, H.M., Ha, C.S., 2013. Bio-nanocomposites for food packaging applications. *Prog. Polym. Sci.* <https://doi.org/10.1016/j.progpolymsci.2013.05.008>.
- Saheb, D.N., Jog, J.P., 1999. Natural fiber polymer composites: a review. *Adv. Polym. Technol.* 18, 351–363. [https://doi.org/10.1002/\(SICI\)1098-2329\(199924\)18:4<351::AID-ADV6>3.0.CO;2-X](https://doi.org/10.1002/(SICI)1098-2329(199924)18:4<351::AID-ADV6>3.0.CO;2-X).
- Sánchez-Safont, E.L., Aldureid, A., Lagarón, J.M., Gámez-Pérez, J., Cabedo, L., 2018. Biocomposites of different lignocellulosic wastes for sustainable food packaging applications. *Compos. Part B Eng.* 145, 215–225. <https://doi.org/10.1016/j.compositesb.2018.03.037>.
- Shi, Y., Ge, Y., Chang, J., Shao, H., Tang, Y., 2013. Garden waste biomass for renewable and sustainable energy production in China: potential challenges and development. *Renew. Sustain. Energy Rev.* 22, 432–437. <https://doi.org/10.1016/j.rser.2013.02.003>.
- Singh, S., Gupta, B., 2016. Physicochemical characteristics of glycerol-plasticized dextran/soy protein isolate composite membranes. *J. Appl. Polym. Sci.* 133. <https://doi.org/10.1002/app.43847>.
- Som, M.-P., Lemée, L., Ambles, A., 2009. Stability and maturity of a green waste and biowaste compost assessed on the basis of a molecular study using spectroscopy thermal analysis thermodesorption and thermochemolysis. *Bioresour. Technol.* 100, 4404–4416. <https://doi.org/10.1016/j.biortech.2009.04.019>.

- Sukhija, S., Singh, S., Riar, C.S., 2016. Analyzing the effect of whey protein concentrate and psyllium husk on various characteristics of biodegradable film from lotus (*Nelumbo nucifera*) rhizome starch. *Food Hydrocoll.* 60, 128–137. <https://doi.org/10.1016/j.foodhyd.2016.03.023>.
- Technical Committee 1–48, 2004. Colorimetry, CIE15 Technical Report. International Commission on Illumination.
- The European Parliament and the Council of the European Union, 2008. Directive 2008/98/EC of the European Parliament and of the Council of 19 november 2008 on waste. . *J. Eur. Union* 9, 3–30.
- Ufodike, C.O., Eze, V.O., Ahmed, M.F., Oluwalowo, A., Park, J.G., Okoli, O.I., Wang, H., 2020. Evaluation of the inter-particle interference of cellulose and lignin in lignocellulosic materials. *Int. J. Biol. Macromol.* 147, 762–767. <https://doi.org/10.1016/j.ijbiomac.2020.01.234>.
- Uitto, J.M., Verbeek, C.J.R., Bengoechea, C., 2020. Shear and extensional viscosity of thermally aggregated thermoplastic protein. *J. Appl. Polym. Sci.* 137, 49393.
- Vandecasteele, B., Boogaerts, C., Vandaele, E., 2016. Combining woody biomass for combustion with green waste composting: effect of removal of woody biomass on compost quality. *Waste Manag.* 58, 169–180. <https://doi.org/10.1016/j.wasman.2016.09.012>.
- Verbeek, R.C.J., van den Berg, L.E., 2010. Extrusion processing and properties of protein-based thermoplastics. *Macromol. Mater. Eng.* 295, 10–21. <https://doi.org/10.1002/mame.200900167>.
- Viretto, A., Gontard, N., Angellier-Coussy, H., 2021. Urban parks and gardens green waste: a valuable resource for the production of fillers for biocomposites applications. *Waste Manag.* 120, 538–548. <https://doi.org/10.1016/j.wasman.2020.10.018>.
- Wei, Y., Li, J., Shi, D., Liu, G., Zhao, Y., Shimaoka, T., 2017. Environmental challenges impeding the composting of biodegradable municipal solid waste: a critical review. *Resour. Conserv. Recycl.* 122, 51–65. <https://doi.org/10.1016/j.resconrec.2017.01.024>.
- Zaini, M.J., Fuad, M.Y.A., Ismail, Z., Mansor, M.S., Mustafah, J., 1996. The effect of filler content and size on the mechanical properties of polypropylene/oil palm wood flour composites. *Polym. Int.* 40, 51–55. [https://doi.org/10.1002/\(sici\)1097-0126\(199605\)40:1<51::aid-pi514>3.3.co;2-9](https://doi.org/10.1002/(sici)1097-0126(199605)40:1<51::aid-pi514>3.3.co;2-9).